Human Molecular Genetics, 2005, Vol. 14, No. 9 ***1183–1197***
doi:10.1093/hmg/ddi129
Advance Access published on March 16, 2005

RPGR ORF15 isoform co-localizes with RPGRIP1 at centrioles and basal bodies and interacts with nucleophosmin

X. Shu[1], A.M. Fry[2], B. Tulloch[1], F.D.C. Manson[1,†], J.W. Crabb[3], H. Khanna[4], A.J. Faragher[2], A. Lennon[1], S. He[4], P. Trojan[5], A. Giessl[5], U. Wolfrum[5], R. Vervoort[1], A. Swaroop[4] and A.F. Wright[1,*]

[1]MRC Human Genetics Unit, Western General Hospital, Edinburgh EH4 2XU, UK, [2]Department of Biochemistry, University of Leicester, Leicester LE1 7RH, UK, [3]Cole Eye Institute and Lerner Research Institute, Cleveland Clinic Foundation, Cleveland, OH, USA, [4]Departments of Ophthalmology and Human Genetics, W.K. Kellogg Eye Center, University of Michigan, Ann Arbor, MI, USA and [5]Institute for Zoology, Johannes Gutenberg-University, Mainz, Germany

Received November 14, 2004; Revised February 18, 2005; Accepted March 10, 2005

The ORF15 isoform of RPGR ($RPGR^{ORF15}$) and RPGR interacting protein 1 (RPGRIP1) are mutated in a variety of retinal dystrophies but their functions are poorly understood. Here, we show that in cultured mammalian cells both $RPGR^{ORF15}$ and RPGRIP1 localize to centrioles. These localizations are resistant to the microtubule destabilizing drug nocodazole and persist throughout the cell cycle. RPGR and RPGRIP1 also co-localize at basal bodies in cells with primary cilia. The C-terminal (C2) domain of $RPGR^{ORF15}$ ($ORF15^{C2}$) is highly conserved across 13 mammalian species, suggesting that it is a functionally important domain. Using matrix-assisted laser desorption ionization time-of-flight mass spectrometry, we show that this domain interacts with a 40 kDa shuttling protein nucleophosmin (NPM). The $RPGR^{ORF15}$–NPM interaction was confirmed by (i) yeast two-hybrid analyses; (ii) binding of both recombinant and native HeLa cell NPM to $RPGR^{ORF15}$ fusion proteins *in vitro*; (iii) co-immunoprecipitation of native NPM, $RPGR^{ORF15}$ and RPGRIP1 from bovine retinal extracts and of native HeLa cell NPM and transfected $RPGR^{ORF15}$ from cultured cells and (iv) co-localization of NPM and $RPGR^{ORF15}$ at metaphase centrosomes in cultured cells. NPM is a multifunctional protein chaperone that shuttles between the nucleoli and the cytoplasm and has been associated with licensing of centrosomal division. RPGR and RPGRIP1 join a growing number of centrosomal proteins involved in human disease.

INTRODUCTION

The ORF15-containing isoform of the RPGR protein ($RPGR^{ORF15}$) is mutated in a variety of retinal dystrophies, including X-linked forms of retinitis pigmentosa (1–6), cone dystrophy (1,7), cone–rod dystrophy (8,9), atrophic macular dystrophy (10) and a syndromal form of retinitis pigmentosa (RP) and recurrent respiratory infections with or without sensorineural hearing loss (11,12). Naturally occurring mutations in $RPGR^{ORF15}$ are also found in two independent breeds of dog with progressive retinal atrophy (13). ORF15 is an alternatively spliced C-terminal exon of *RPGR*, which is expressed in a variety of human tissues but is most abundant in the retina in all species examined (1,13–18).

In the mouse retina, RPGR protein is associated with the connecting cilium of rod and cone photoreceptors, which connects the inner and outer segments (15); this is also the case in humans and other mammalian species, but it is unclear whether it is also expressed in photoreceptor outer segments (17,18). An *Rpgr* knockout mouse shows a progressive degeneration of cone and rod photoreceptors and is associated with mislocalization of opsin-containing vesicles (15). These

*To whom correspondence should be addressed. Email: alan.wright@hgu.mrc.ac.uk
†Present address: Centre for Molecular Medicine, The University of Manchester, Oxford Road, Manchester M13 9PT, UK.

vesicles are normally transported to the base of the connecting cilium by means of the minus-end directed microtubule-associated motor protein cytoplasmic dynein (19). Here, they fuse with the plasma membrane before being transported along the ciliary plasma membrane by plus-end directed microtubule motors such as kinesin-II to the photoreceptor outer segment (20).

The function of RPGR is unclear although structural alignment of the N-terminal half of RPGR (exons 1–11) with RCC1, a guanine nucleotide exchange factor (GEF) for the small GTPase Ran (21–23), suggests a role in the regulation of small GTPases. However, RPGR has not been shown to have GEF activity with Ran. Yeast two-hybrid screening of retinal libraries has shown that the RCC1-like domain ($RPGR^{RLD}$) binds a novel protein of unknown function, RPGR interacting protein 1 (RPGRIP1) (24–27). Loss-of-function mutations in *RPGRIP1* cause a form of congenital retinal blindness, Leber's congenital amaurosis (28–29) and a later onset cone–rod dystrophy (30). RPGRIP1 also localizes to the connecting cilium of rod and cone photoreceptors and an *Rpgrip1* knockout mouse shows progressive degeneration of rod and cone photoreceptors, with abnormal extended outer segment discs and an inability to localize RPGR to the connecting cilium (27).

The C-terminal half of the RPGR-ORF15 isoform contains a highly repetitive glutamic acid-rich plaid domain, which is a mutation hotspot, plus a non-repetitive and basic ORF15 C-terminal domain ($ORF15^{C2}$) that is reported to be conserved among human, mouse, bovine and *Fugu* fish (1). The latter observation suggested that $ORF15^{C2}$ may have an important functional role. Here we show that the $ORF15^{C2}$ domain of $RPGR^{ORF15}$ interacts and co-localizes with nucleophosmin (NPM or B23). Furthermore, $RPGR^{ORF15}$ co-localizes with RPGRIP1 at centrioles and basal bodies of cultured mammalian cells.

RESULTS

Conservation of $ORF15^{C2}$

We first determined the extent of cross-species conservation of the C-terminal (C2) region of $RPGR^{ORF15}$ ($ORF15^{C2}$), defined by a clone containing the C-terminal 83 amino acids of human $RPGR^{ORF15}$ (residues 1070–1152; GenBank accession nos AF286472 and AAC50481), which marks a relatively abrupt change in sequence composition from the acidic glutamic acid-rich 'plaid' domain to the basic C-terminal domain (1) (Fig. 1A and B). This was investigated by sequencing the $ORF15^{C2}$ region in 13 different species, comprising primates (human, gorilla, rhesus monkey, marmoset), rodents (mouse, rat, hamster), carnivores (cat, dog), artiodactyls (cow, pig, sheep) and fish (*Fugu rubripes*). The results (Fig. 1B) show that amino acid sequence identity within the C2 domain is high across all species, with the exception of *F.rubripes*, in which identity was confined to the most C-terminal 30 amino acids. The identity of human RPGR was highest with gorilla (96% identity) followed by marmoset (90%), rhesus monkey (87%), cow and cat (64%), sheep (63%), dog and pig (62%), hamster (55%), rat (51%), mouse (45%) and *F. rubripes* (21%). The high degree of conservation supports the view that $ORF15^{C2}$ is a functional domain.

Identification of NPM in protein pull-down experiments

A fusion protein containing the C-terminal 81 amino acids of bovine $RPGR^{ORF15}$ ($bORF15^{C2}$) fused to glutathione-*S*-transferase (GST) was immobilized onto glutathione–Sepharose beads and used to pull down $ORF15^{C2}$-interacting proteins from bovine retinal and kidney extracts. Eluted proteins were separated by sodium dodecyl sulphate–polyacrylamide gel electrophoresis (SDS–PAGE), and retinal extract bands that were not present in the GST vector-only control were excised, and following in-gel digestion with trypsin, peptide mass mapping was performed using matrix-assisted laser desorption ionization time-of-flight (MALDI-TOF) mass spectrometry. One of the excised bands of mass 40 kDa from the retinal pull-down was identified as NPM by MALDI-TOF (Fig. 1C). The same band was prominent (but not analysed by mass spectrometry) in kidney. Other excised bands were identified as cleavage products of GST, bovine adenine nucleotide translocase, actin, β-tubulin, eukaryotic translation elongation factor 1 gamma, pre-procollagenase and glutamate dehydrogenase. Further work was carried out on the putative interaction of $ORF15^{C2}$ with NPM. The interaction of ORF15 with NPM was initially confirmed by immunoblotting using anti-NPM antibody following GST–$bORF15^{C2}$ pull down from bovine retinal extracts (Fig. 1D).

Human RPGR $ORF15^{C2}$ was used as 'bait'(pAS vector) and human NPM as 'prey' (pACT vector) to test for interaction in a yeast two-hybrid analysis. A positive interaction between NPM and $hORF15^{C2}$ was shown by the ability to grow on triple selection plates lacking tryptophan (−Trp), leucine (−Leu) and histidine (−His) (Fig. 1E). This was confirmed by testing the ability of putative interacting clones to metabolize X-gal with β-galactosidase, as shown by formation of blue colour (data not shown).

Additional pull-down experiments were carried out using both native NPM in HeLa cell extracts and recombinant NPM. HeLa cell extracts were incubated *in vitro* with a purified GST human $ORF15^{C2}$ fusion protein (GST–$hORF15^{C2}$) and GST control. After washing and elution from glutathione–Sepharose beads, interacting proteins were analysed by SDS–PAGE and western blots. This confirmed that native NPM from crude HeLa supernatant binds to $hORF15^{C2}$ *in vitro* (Supplementary Material, Fig. S1A). Recombinant human NPM was also incubated with GST–$hORF15^{C2}$ *in vitro* and, after affinity purification and washing, analysis of the eluted products showed that recombinant NPM also binds $hORF15^{C2}$ (Supplementary Material, Fig. S1B).

The possibility of non-specific interaction between the basic ORF^{C2} peptide (pI = 9.64) and the acidic NPM (pI = 4.64) was excluded by testing for interaction between the protein 14-3-3 (pI = 4.63) and GST-tagged $ORF15^{C2}$ by protein pull-down experiments. Cell extracts from the human embryonic kidney (HEK) 293 cell line, which express both 14-3-3 and NPM as native proteins, were incubated with GST–$ORF15^{C2}$ and GST control beads. The bound proteins were screened by western blotting using anti-14-3-3 antibody (full-length isoform) and anti-NPM. This showed no interaction between 14-3-3 and $ORF15^{C2}$ but confirmed the interaction with NPM (Supplementary Material, Fig. S1C). A similar experiment with recombinant enhanced green fluorescent protein

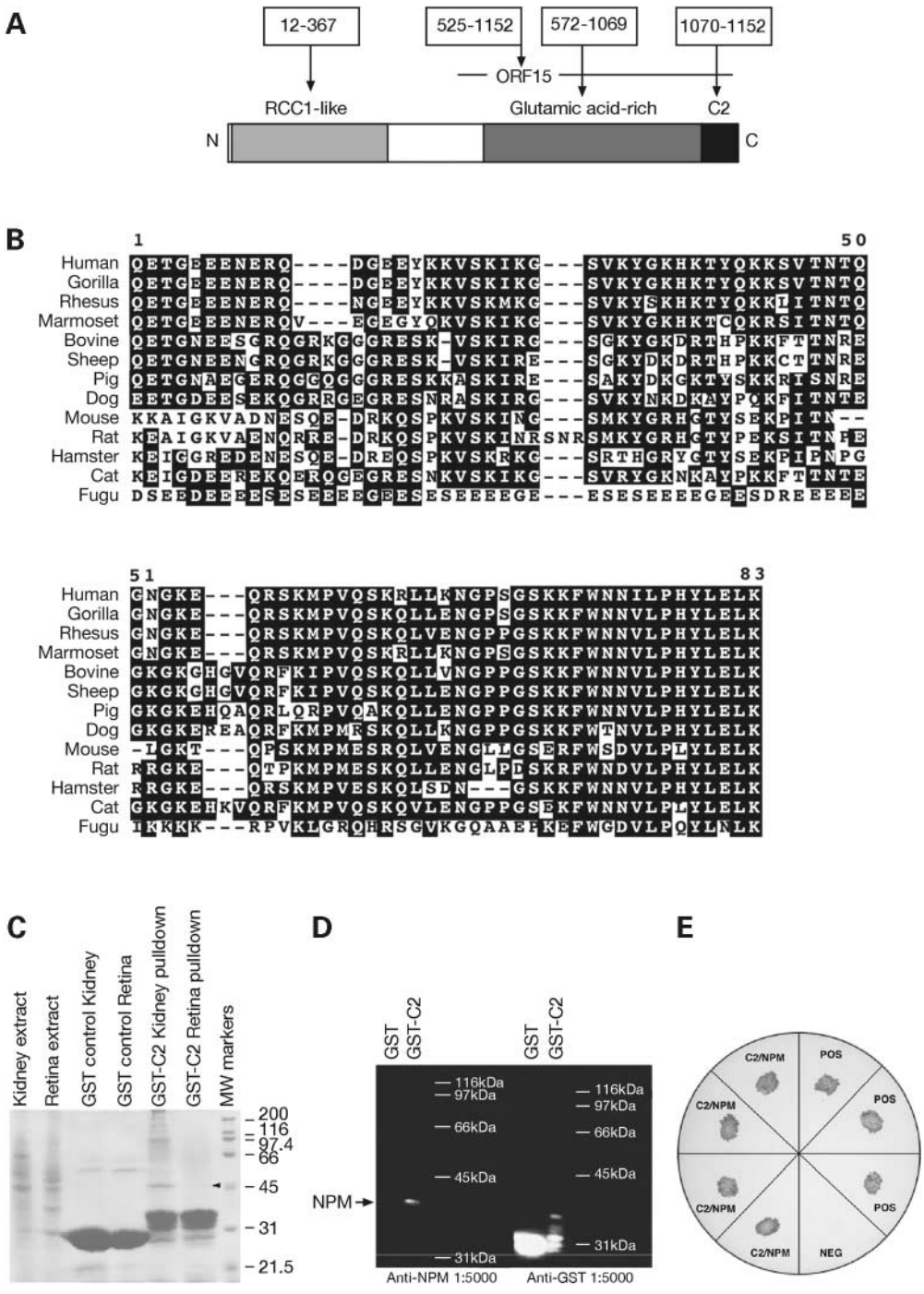

Figure 1. (**A**) Schematic structure of RPGR^{ORF15} protein (drawn to scale). The N- and C-termini and RCC1-like, glutamic acid-rich and ORF15^{C2} (C2) domains are shown (with their residue numbers) and the product of exon ORF15, which includes over half of the final protein, is indicated by a line (based on RPGR accession nos AF286472 and AAC50481). (**B**) Conservation of RPGR^{ORF15} C-terminal (ORF15^{C2}) region in 13 different species. The amino acid sequence of each species is shown below the C-terminal 83 amino acids (residues 1070–1152) of human RPGR^{ORF15} (which defines C2) after alignment using CLUSTALW. Identical residues are shown as boxed in black. Accession nos used for RPGR ORF15 were: AF286472 (human); AY855163 (gorilla); AY855162 (rhesus); AY855164 (marmoset); AF286474 (bovine); Y855169 (sheep); AY855167 (pig); AF385629 (dog); AF286473 (mouse); AY855168 (rat); AY855166 (hamster); AY855167 (cat) and AF286475(*Fugu*). (**C**) Protein pull-down using GST–bORF15^{C2} (GST–C2) with bovine retinal and kidney extracts leading to the identification of NPM, as an interacting protein. Coomassie Blue-stained PAGE gel is shown containing retinal and kidney extract proteins prior to (5% of input extract) and after pull down with GST–bORF15^{C2} (GST–C2) when compared with GST-only controls. The 40 kDa NPM band is indicated by an arrowhead. The major bands are GST and GST–C2. (**D**) The ORF15^{C2}-interacting band is further identified as NPM (arrowed) with anti-NPM antibody after a protein pull-down experiments using GST–bORF15^{C2} (GST–C2) and bovine retinal extract, compared with GST-only control (GST). The results are compared with anti-GST antibody. Molecular weight size standards (in kilodalton) and antibody dilutions are shown beside each gel. (**E**) Interaction of ORF15^{C2} (C2) and NPM shown by yeast two-hybrid analysis (in quadruplicate), based on triple nutrient selection (medium lacking tryptophan, leucine and histidine), when compared with positive (POS) and negative (NEG) control plasmids.

(EGFP) (pI = 5.8) also failed to show interaction with ORF15^{C2} (data not shown), supporting the specificity of the ORF15^{C2}–NPM interaction.

Co-immunoprecipitation of NPM and RPGR^{ORF15}

To further corroborate the interaction between NPM and RPGR^{ORF15}, HeLa cells were transfected with constructs expressing EGFP fused to hORF15^{C2} (EGFP–hORF15^{C2}) or with an EGFP control plasmid. Anti-EGFP antibody was used to co-immunoprecipitate native NPM with EGFP–hORF15^{C2} (Fig. 2A). A minor NPM band with slightly lower molecular weight was also identified, perhaps representing a post-translational modification or degradation product.

In order to test whether anti-ORF15^{C2} antibody can co-immunoprecipitate native NPM from retina, bovine retinal rod outer segment (ROS) fractions were incubated with antibody and, after washing, the immunoprecipitated fraction was separated by SDS–PAGE and western blots probed with anti-ORF15^{C2}, anti-RPGRIP1 and anti-NPM antibodies. The results (Fig. 2B) show that RPGR^{ORF15}, RPGRIP1 and NPM are each co-immunoprecipitated from retina by anti-ORF15^{C2} antibody (but not by pre-immune serum or protein A–Sepharose beads).

NPM is predominantly present in nucleoli (31). We therefore tried to determine whether RPGR^{ORF15} forms part of a nuclear complex with NPM *in vivo*. Two different antibodies (anti-ORF15^{C2} and anti-ORF15^{CP}) were used in co-immunoprecipitation experiments using bovine retinal nuclear extract (RNE). Immunoblot analysis of immunoprecipitates detected anti-NPM immunoreactive bands of the expected size, ~40 kDa (Fig. 2C). NPM was not immunoprecipitated when normal rabbit IgG was used as control. However, reverse co-immunoprecipitation experiments with anti-NPM antibody did not reveal RPGR^{ORF15} upon immunoblot analysis using ORF15 antibodies (data not shown). This is probably because of low amounts of RPGR^{ORF15} in the NPM-containing multiprotein complex(es) in the retina. Similar sized RPGR^{ORF15} protein bands were detected in RNE with both anti-ORF15 antibodies but the nuclear band was slightly smaller than the major bands seen in whole retinal extracts, suggesting the presence of a distinct nuclear isoform, which showed substantial (50–100-fold) enrichment in nuclei (Fig. 2E). We also found a punctate pattern of nuclear labelling in cell lines using anti-RPGR^{ORF15} antibody in cultured cells, which was absent from cells labelled with pre-immune serum (Fig. 2D).

Co-localization of RPGR^{ORF15} and RPGRIP1 at centrosomes in cultured mammalian cells

Antibodies raised against the bovine ORF15^{C2} domain (anti-bORF15^{C2}) and against a synthetic peptide (1878) from a non-repetitive region of human ORF15 (anti-hORF15^{1878}) were used in indirect immunofluorescence microscopy experiments to determine the subcellular localization of both the transfected and the native RPGR^{ORF15} isoform in a variety of cultured cells. The expression of RPGR^{ORF15} was first examined in cultured mammalian cells using reverse transcriptase–polymerase chain reaction (RT–PCR) (Supplementary Material, Fig. S1D). This confirmed equivalent expression of *RPGR*^{ORF15} transcripts across cell lines, when compared with the constitutively expressed enzyme glyceraldehyde-3-phosphate dehydrogenase (GAPD).

COS7 cells were transfected with a vector expressing EGFP–bORF15^{C2} fusion protein and analysed by fluorescence microscopy. Transfected cells could be identified by green fluorescence which co-localized with anti-NPM antibody in nucleoli (Fig. 3A). Constructs expressing the entire exon ORF15 were not detected in the nucleus, presumably because their size exceeds the nuclear pore diffusion limit and RPGR^{ORF15} does not have appear to have a nuclear localization signal (NLS).

The localization of native RPGR^{ORF15} was examined in cultured cells expressing RPGR^{ORF15}. Two different anti-ORF15 antibodies (anti-1878 and anti-ORF15^{C2}) co-localized with γ-tubulin in U2OS and HeLa cell lines, consistent with a centrosomal localization (Fig. 3B). In certain views, it appeared that the RPGR labelling of the centrosomes formed a crescent or annular appearance (Fig. 3B, inset). Co-localization of RPGR^{ORF15} with centrosomes was observed in all five cell lines examined—HeLa, U2OS, NIH 3T3, ARPE-19 and COS7—using both anti-ORF15 antibodies. High-resolution imaging revealed two pairs of fluorescent dots in cells in G2 phase of the cell cycle, which was consistent with a specific centriolar localization (Fig. 3C). Localization of RPGR^{ORF15} in mitotic cells revealed spindle pole labelling from prophase through to telophase (Fig. 3D).

The dependence of RPGR^{ORF15} centrosomal localization on microtubule polymerization was examined by culturing cells in the presence and absence of the microtubule destabilizing agent nocodazole. Staining with anti-bORF15^{C2} and α-tubulin antibodies showed that ORF15 staining of centrosomes was resistant to treatment with nocodazole, hence it was not dependent on the presence of an intact microtubule network (Fig. 4).

Since RPGR interacts with RPGRIP1, and the ciliary localization of RPGR is dependent on the presence of RPGRIP1, two different antibodies to RPGRIP1 were tested in the same cell lines for co-localization with RPGR by indirect immunofluorescence microscopy. The results show that both RPGRIP1 antibodies co-localized with γ-tubulin in U2OS cells consistent with a centrosomal localization (Fig. 4). High resolution imaging again revealed two pairs of fluorescent dots in prophase cells consistent with centriolar localization (Fig. 4). Staining with anti-RPGRIP1 and α-tubulin antibodies showed that RPGRIP1 staining of centrosomes was again resistant to treatment with nocodazole and not dependent on microtubule polymerization (Fig. 4).

The co-localization of native RPGR^{ORF15} and NPM was investigated in cultured mammalian cells using indirect immunofluorescence microscopy (Fig. 5). In both HeLa and U2OS cells, NPM was detected exclusively in nucleoli during interphase, but co-localized with spindle poles in mitosis. This falls in line with previous studies that NPM is a nucleolar protein (31), but that at mitosis it can associate with spindle poles (32). However, in contrast to this latter study (32), we could not detect NPM at interphase centrosomes in an asynchronous population of cells. The spindle pole association of NPM precisely overlapped with the RPGR^{ORF15} signal during

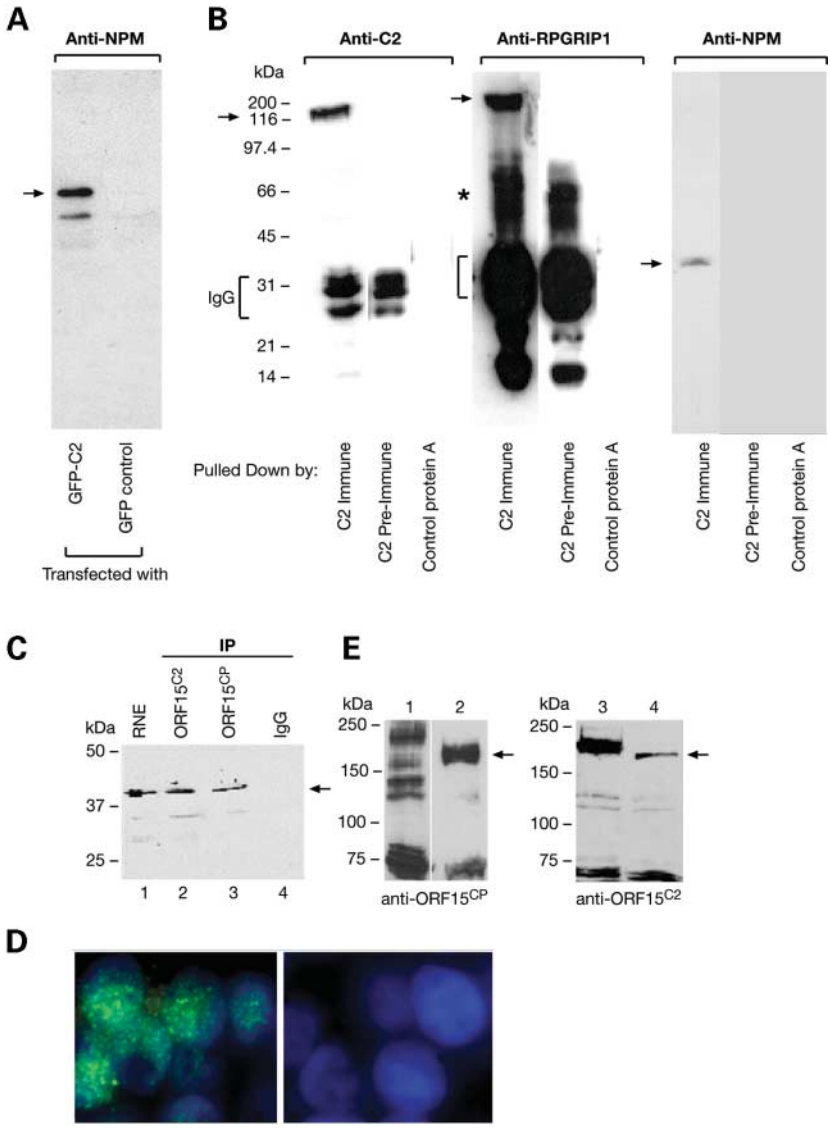

Figure 2. Co-immunoprecipitation of native NPM from HeLa cells and bovine retinal extracts. (**A**) Co-immunoprecipitation of native NPM in HeLa cell extracts after transfection with EGFP–ORF15^{C2} (GFP–C2), using anti-EGFP antibody, compared with EGFP-only (GFP) and protein A–Sepharose bead controls, probed with anti-NPM, showing a major 40 kDa band and a smaller band. (**B**) Co-immunoprecipitation of RPGR^{ORF15} with NPM and RPGRIP1 from a bovine retinal (ROS) fraction, using anti-ORF15^{C2} (anti-C2) antibody. Precipitated proteins (filled arrows) were detected using anti-C2, anti-RPGRIP1 and anti-NPM antibodies. Immunoglobulin bands are indicated by brackets and unknown contaminants by the asterisk. (**C**) Co-immunoprecipitation of RPGR and NPM from bovine RNE. Bovine RNE (500 μg) was incubated with anti-ORF15^{C2}, anti-ORF15^{CP} or normal rabbit immunoglobulin (IgG) as indicated. The immunoprecipitated proteins were analyzed by SDS–PAGE followed by immunoblotting using anti-NPM antibody. RNE lane was loaded with 20 μg of protein (4% of input). The molecular weight of marker proteins is shown in kilodalton. The arrow indicates the NPM immunoreactive band. Molecular weight markers are indicated on the left in kilodalton. (**D**) Immunoflorescence labelling of human ARPE-19 cell nuclei with anti-RPGR^{OREF15} (1878) antibody (left frame) compared with pre-immune serum (right frame). RPGR^{ORF15} shows a punctate pattern of nuclear labelling. (**E**) Immunoblot analysis of the bovine RNE with ORF15^{CP} and ORF15^{C2} antibodies. Bovine retinal whole cell extract (lanes 1 and 3) and nuclear extract (lanes 2 and 4) (100–200 μg each) were subjected to SDS–PAGE followed by immunoblotting using anti-ORF15^{CP} (lanes 1, 2) or anti-ORF15^{C2} (lanes 3, 4) antibody. Arrows indicate the RPGR immunoreactive bands recognized by the antibodies in the nuclear fractions. Molecular weight markers are indicated on the left in kilodalton.

metaphase but not during anaphase, when the two signals were slightly separated (Fig. 5A). During metaphase, the NPM signal extended outside of the RPGR^{ORF15} signal, in a triangular pattern of labelling, suggesting labelling of centrosomal satellites (33). In contrast, γ-tubulin and RPGR^{ORF15} co-localized precisely at all stages of mitosis (Fig. 5B).

NPM immunofluorescence in the retina

In order to examine the localization of NPM in retina, bovine retinal sections were examined for NPM immunofluorescence, when compared with the centriolar and basal body protein centrin (34), and with RPGR, which was previously reported

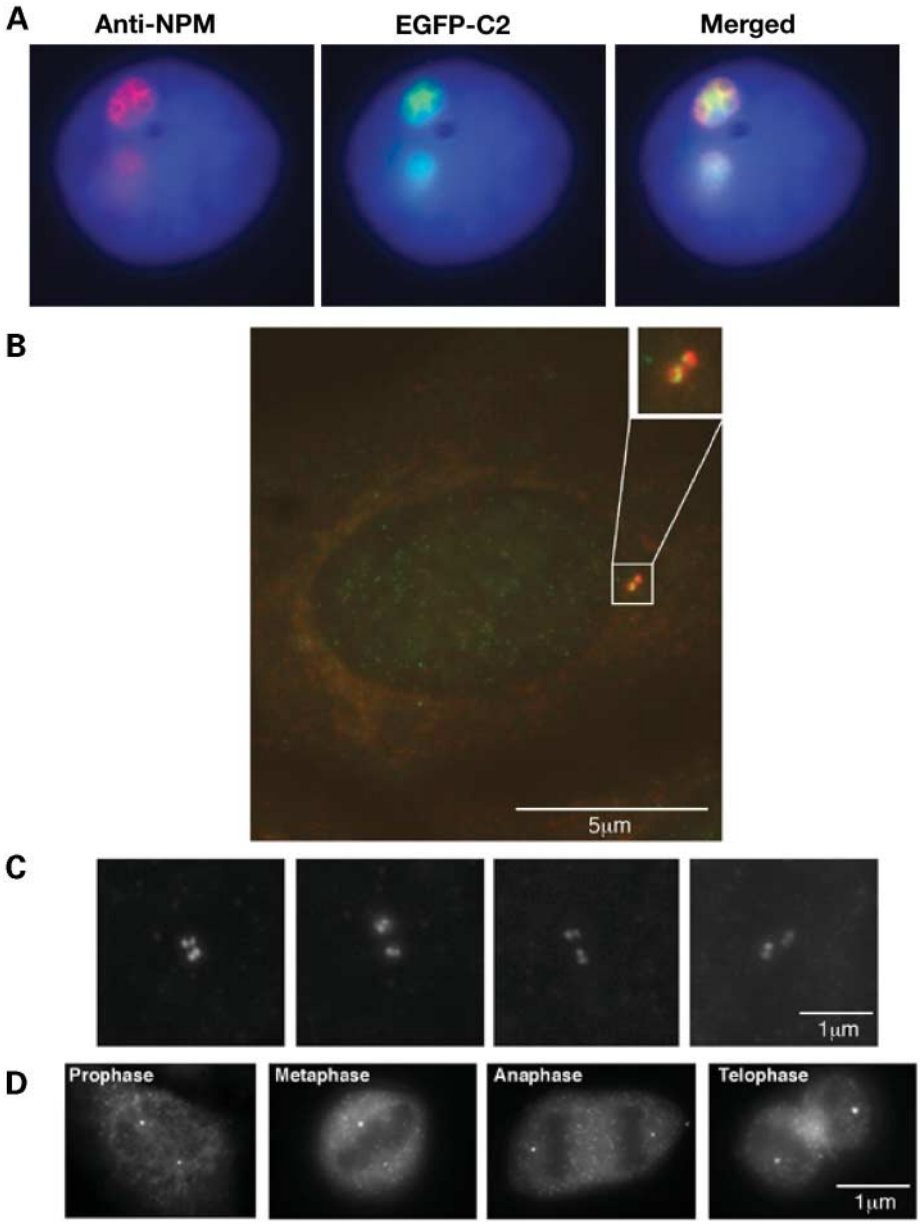

Figure 3. RPGR^{ORF15} localization in human U2OS and HeLa cells. (**A**) Transfected EGFP–hORF15^{C2} co-localizes with NPM in nucleoli of cultured HeLa cells. Larger EGFP–ORF15 constructs did not show nuclear labelling. (**B**) In U2OS cells, antibodies raised against ORF15^{C2} (green) co-localize with antibodies directed against the centrosome-specific component, γ-tubulin (red). An enlarged view of the region containing the centrosome is shown in the inset. Note the apparent crescent-shaped labelling with anti-ORF15^{C2} antibody. (**C**) High-resolution images of centrosomes in U2OS (first three panels) or HeLa (fourth panel) cells labelled with anti-bORF15^{C2} antibodies. The cells shown have already undergone centrosome duplication and two pairs of centrioles are detected by the anti-bORF15^{C2} antibodies indicating that RPGR^{ORF15} is a centriolar, rather than PCM, component. (**D**) RPGR^{ORF15} is present at the centrosome at all stages of mitosis in U2OS cells. Prophase, metaphase, anaphase and telophase cells are shown in which spindle poles are detected with anti-bORF15^{C2} antibodies. No staining of other spindle structures or mitotic chromosomes is detected using anti-ORF15^{C2} antibody. Scale bars are indicated for b–d.

to label connecting cilia but not basal bodies (18). The results (Fig. 6) showed strong centrin and RPGR signals, but no NPM signal, in the region of photoreceptor connecting cilia. Photoreceptor outer segments are also labelled with anti-RPGR^{ORF15} antibody (Fig. 6B). NPM immunofluorescence was detected in a punctate distribution within each nuclear layer, consistent with nucleolar localization, which was most marked in ganglion cells. A nuclear localization for RPGR was evident in cultured cells (Fig. 2D) but not in retinal sections unless antigen retrieval methods were used (unpublished data). Failure to detect NPM in photoreceptor connecting cilia or basal bodies is probably because it is only present in the centrosomes of mitotic cells.

RPGR and RPGRIP1 co-localize in basal bodies

Quiescent mouse inner medullary collecting ductal epithelial (IMCD3) cells possess primary cilia growing from basal

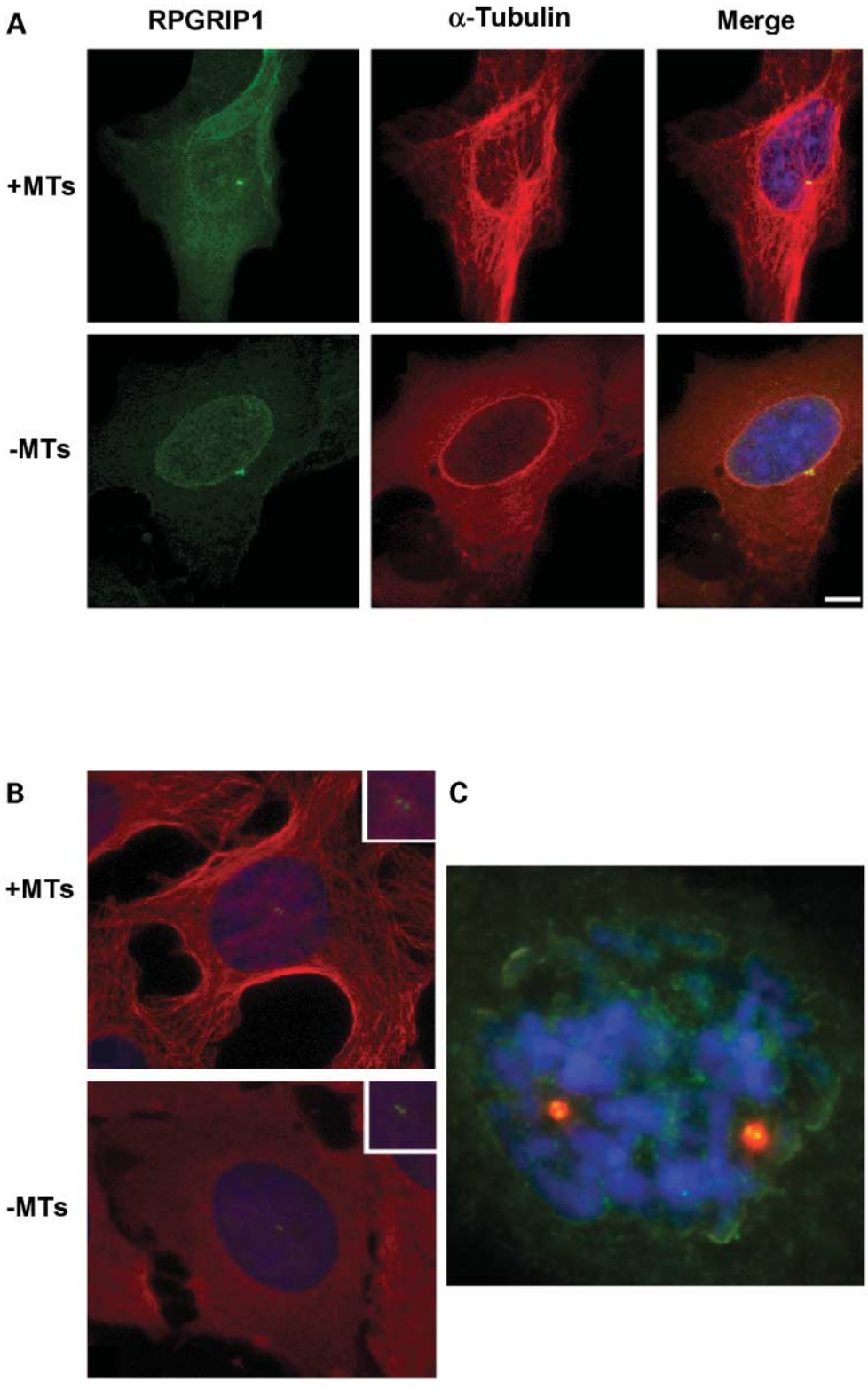

Figure 4. Staining of centrioles with anti-ORF15^{C2} and anti-RPGRIP1 antibodies is independent of microtubule polymerization. **(A)** Immunolocalization of RPGRIP1 at centrosomes in a microtubule-independent manner. Human U2OS cells were either untreated (+MTs) or treated (−MTs) with 6 mg/ml nocodazole to depolymerize microtubules. Following fixation, cells were labelled with antibodies against RPGRIP1 (green) and α-tubulin (red) and nuclei stained with DAPI (blue). Merged images including nuclei (DAPI, blue) are shown. (**B**) An interphase U2OS cell is labelled with anti-α-tubulin (red) and anti-ORF15^{C2} (green) in the absence (+MTs) and presence (−MTs) of the microtubule depolymerizing agent nocodazole. Labelling of centrioles is seen to be resistant to nocodazole. The DNA is stained blue by DAPI. (**C**), An enlarged view of a prophase cell labelled as described earlier. Note that RPGRIP1 forms two discrete dots representative of centrioles (yellow) within each spindle pole.

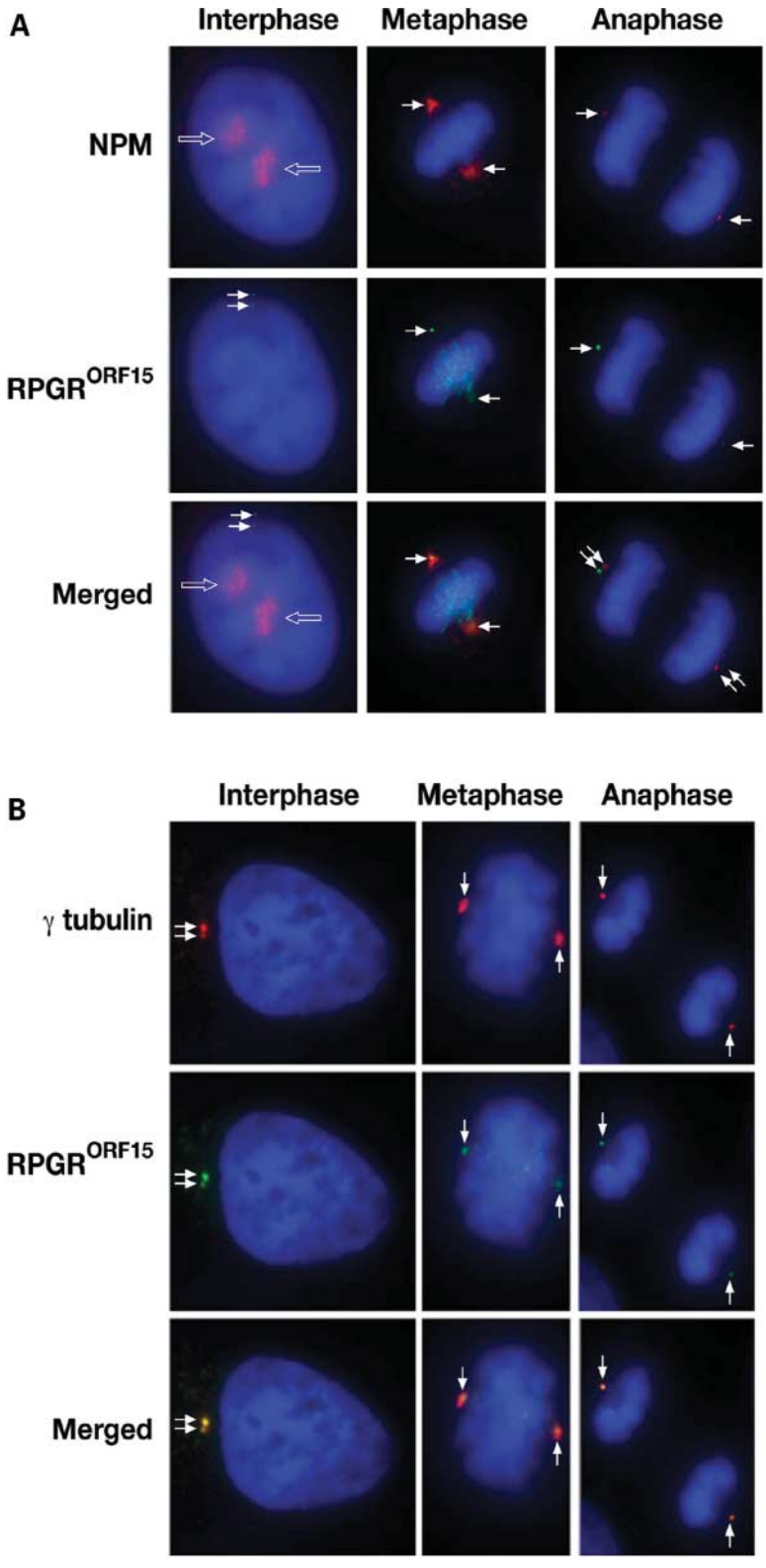

Figure 5. Co-localization of NPM and RPGR^{ORF15} at centrosomes in mitotic cells during metaphase. (**A**) Cell cycle stages in ARPE-19 cells analysed by indirect immunofluorescence, using anti-NPM (red) and anti-ORF15^{C2} (green) antibodies. The NPM signal is located at centrosomes in metaphase (closed arrows), in nucleolar granules during interphase (open arrows) and adjacent to centrosomes in anaphase (closed arrows). RPGR^{ORF15} is located at centrosomes in interphase (which are duplicated in G2), and at the spindle poles during mitosis (metaphase and anaphase) (closed arrows). NPM co-localizes with RPGR^{ORF15} in metaphase but extends beyond the RPGR^{ORF15} signal. (**B**) Co-localization of RPGR^{ORF15} with γ-tubulin (closed arrows) during cell cycle stages in ARPE-19 cells by indirect immunofluorescence, using anti-γ-tubulin (red) and anti-RPGR^{ORF15} (green). RPGR^{ORF15} overlaps with γ-tubulin at all stages of the cell cycle.

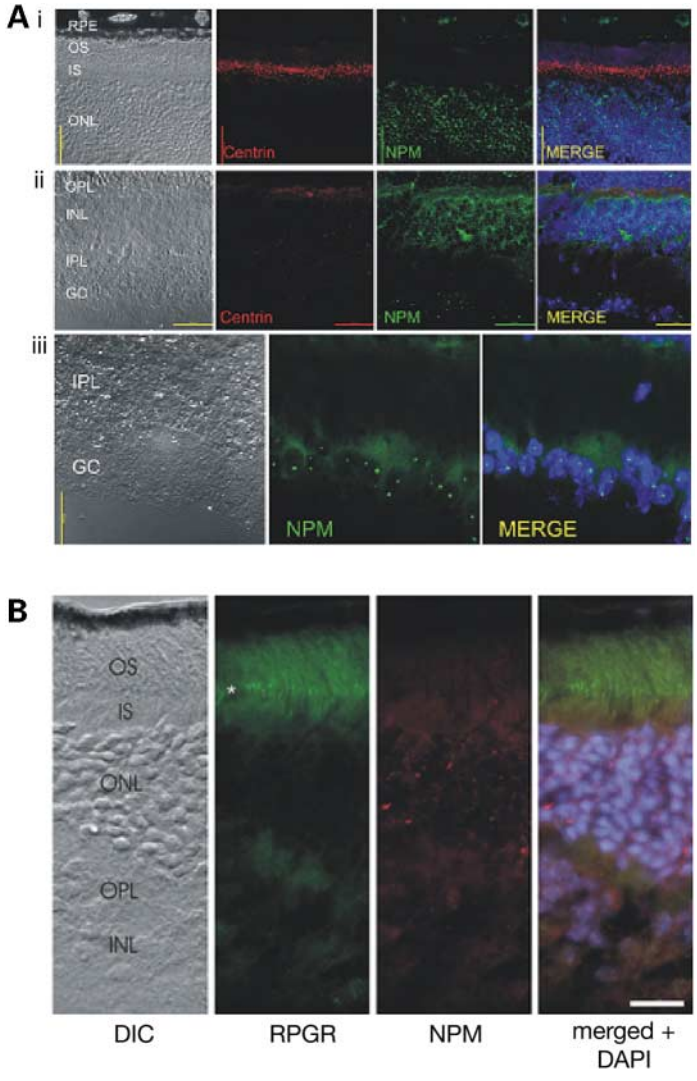

Figure 6. Localization of NPM and RPGR^{ORF15} in mouse retinal layers by indirect immunofluorescence. (**A**) Mouse retinal sections are labelled with anti-centrin antibodies (red) (i, ii) and anti-NPM (green) (i–iii) and the retinal layers are indicated on the left by differential interference contrast. The connecting cilia and basal bodies are labelled with anti-centrin antibodies while NPM is located in all nuclear layers and shows a punctate staining characteristic of nucleolar labelling, which is most marked in ganglion cell nuclei (iii). The merged images are shown on the right and retinal layers are labelled as follows: RPE, retinal pigment epithelium; OS, photoreceptor outer segments; IS, photoreceptor inner segments; ONL, outer nuclear layer; OPL, outer plexiform layer; INL, inner nuclear layer; IPL, inner plexiform layer; GC, ganglion cell layer. Nuclei are stained with DAPI. (**B**) Double labelling of NPM and RPGR^{ORF15} (anti-NPM and anti-bORF15^{C2} antibodies). NPM is not localized in the connecting cilium or photoreceptor outer segments, where the RPGR^{ORF15} isoform is stained. However, RPGR^{ORF15} is not present in the nucleolus where NPM is found.

bodies which label with anti-acetylated γ-tubulin antibodies. These cells were fixed and used for immunocytochemistry with anti-acetylated γ-tubulin, anti-RPGR^{ORF15} and anti-RPGRIP1 antibodies. The results show that both RPGR and RPGRIP1 co-localize at the basal bodies in IMCD3 cells (Fig. 7).

DISCUSSION

Here, we show for the first time that both RPGR^{ORF15} and RPGRIP1 localize to centrosomes and spindle poles in cultured dividing cells. Centrosomes are complex organelles, which act as the major microtubule organizing centre for the cell (33,35). They consist of two orthogonally aligned, barrel-shaped centrioles, each with a 9+0 microtubule triplet array surrounded by a protein matrix, the pericentriolar material, which is involved in nucleating microtubules. During S/G2 phase, centrosomes duplicate, generating two pairs of centrioles and during mitosis, these pairs separate to form the two spindle poles. In certain post-mitotic differentiated cells, such as photoreceptors, centrioles are repositioned within the cytoplasm and contribute to the growth of cilia. Here, the centrioles are referred to as basal bodies. Although not structurally distinct from centrioles, basal bodies do not appear to recruit pericentriolar material. The older centriole/basal body of the pair sits at the base of the cilium and nucleates the ciliary microtubules from its distal end.

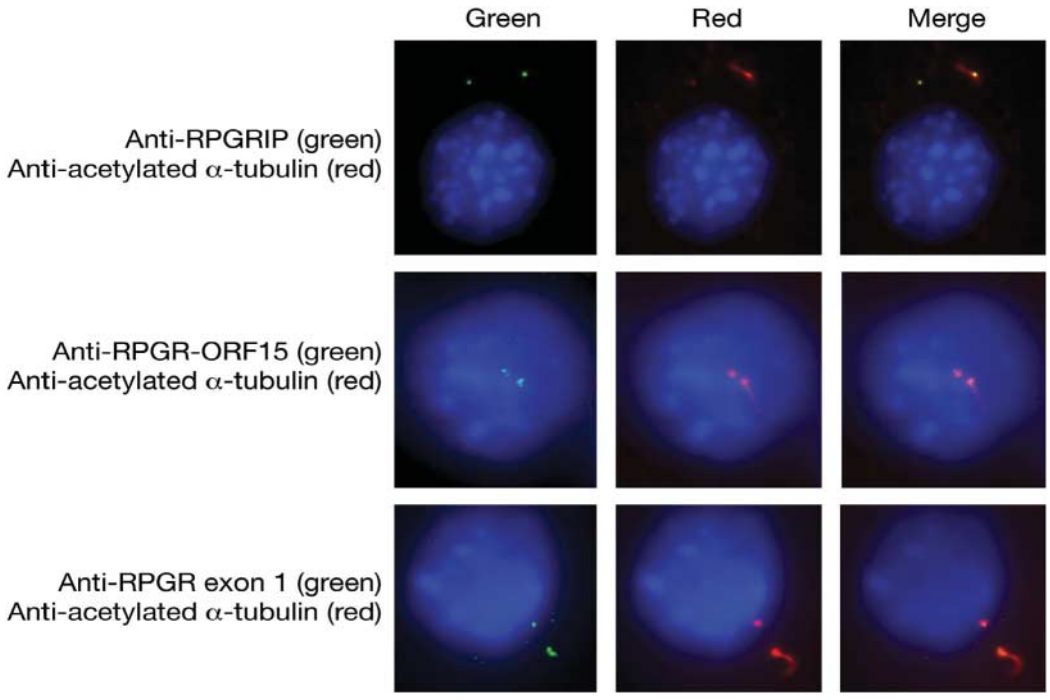

Figure 7. Co-localization of RPGR^{ORF15} and RPGRIP1 at basal bodies in ciliated IMCD3 cells. Quiescent cells are labelled with anti-acetylated α-tubulin (red) and anti-RPGR^{ORF15} (anti-RPGR-ORF15) (green) or anti-RPGRIP1 (anti-RPGRIP) (green) antibodies. Primary cilia, shown as elongated structures, nucleated at one (mother) basal body, and the second (daughter) basal body, all stain red. RPGR^{ORF15} and RPGRIP1 antibodies clearly label both basal bodies (green). Three different cells are shown with individually stained and merged images. Acetylated α-tubulin is present in microtubules, such as primary cilia and basal bodies, that are more stable than the majority of cytoplasmic microtubules.

Both RPGR^{ORF15} and RPGRIP1 localize to centrosomes throughout the cell cycle in all of the non-ciliated cell lines examined, including HeLa, HEK 293, COS7, NIH 3T3 and ARPE-19. Importantly, the detection of both RPGR^{ORF15} and RPGRIP1 in four small punctate structures late in the cell cycle supports the notion that both these proteins are components of centrioles themselves rather than the surrounding pericentriolar material. RPGRIP1 may serve to anchor RPGR^{ORF15} to the centriole in cultured cells, as it does to the ciliary axonemes of photoreceptors. Localization of both RPGR^{ORF15} and RPGRIP1 to centrosomes is not dependent on microtubules, strengthening the hypothesis that these are core centriolar proteins and not proteins localizing to the minus-ends of cytoplasmic microtubules. In the renal medullary cell line IMCD3, which contains primary cilia nucleated by basal bodies, both RPGR^{ORF15} and RPGRIP1 co-localize at the basal bodies. This is consistent with the close relationship between basal bodies and centrioles. Although both proteins have previously been reported to be present in photoreceptor connecting cilia, neither was known to be a component of basal bodies (18).

Interestingly, we also show that RPGR^{ORF15} isoform interacts with the multifunctional molecular chaperone NPM. NPM is a 40 kDa phosphoprotein, which is present in nucleoli and centrosomes at different stages of the cell cycle. In both these locations, protein 'crowding' is significant, and NPM may facilitate specific interactions or prevent protein aggregation and denaturation (31,36–38). It is a member of the nucleoplasmin family of chaperones and has a number of apparently distinct functions, including association with pre-ribosomal particles, binding and cleavage of pre-rRNA, shuttling of ribonucleoprotein and other proteins between nucleus and cytoplasm, binding to NLS-containing proteins and interaction with p53, RB, the nucleolar protein p120, nucleolin and a number of viral proteins (36). It is able to oligomerize, and is found as a hexamer in the nucleolus, although phosphorylated NPM may be monomeric (36).

The interaction of RPGR^{ORF15} and NPM and the co-localization of these two proteins at centrosomes raise the question as to the physiological significance of the interaction. NPM has been suggested to be present at centrosomes from mitosis through to late G1/S (32). We were only able to confirm the presence of NPM at centrosomes during mitosis and specifically during metaphase (Fig. 5A). At this stage, the NPM signal overlaps with RPGR^{ORF15} but extends beyond it, whereas RPGR^{ORF15} is confined to the centrioles. In interphase cells, there was no clear evidence of NPM at centrosomes, whereas there was a strong nucleolar signal. At anaphase, the NPM and RPGR^{ORF15} signals were narrowly separated, suggesting that NPM may be localized to the distal centrosomal satellites (33) or a neighbouring structure. It is not known what proteins anchor NPM to centrosomes but the evidence presented suggests that it is not RPGR^{ORF15}, which overlaps with but does not co-localize with NPM at all stages of the cell cycle.

NPM has been proposed to 'licence' centrosomal duplication in late G1/S phase, in co-ordination with DNA duplication, and is then released from centrosomes in response to

Cdk2/cyclin E-mediated phosphorylation of Thr^{199} (which may be maintained by Cdk2/cyclin A during G2) (36). NPM is thought to re-associate with centrosomes during mitosis, possibly in response to phosphorylation of Thr^{234} and Thr^{237} residues by Cdk1/cyclin B (32). One possibility is that $RPGR^{ORF15}$ and RPGRIP1 associate together at the centrosomes and are involved in the unloading of microtubule transport cargoes at various stages of the cell cycle, one of which includes NPM. In this context, the recent demonstration that Ran is a core centrosomal component which can form Ran–GTP from Ran–GDP at this site (38), raises the question as to whether the RCC1-like domain of $RPGR^{ORF15}$ could act as a GEF for centrosomal Ran, perhaps facilitating the unloading of NPM, which has a NLS and is capable of binding to importin. It has been shown that a number of core centrosomal proteins shuttle between the nucleus and the centrosomes, which is blocked by leptomycin (39). These shuttling proteins are proposed to be released from importin in the presence of centrosomal Ran–GTP, by analogy with the unloading of importin cargoes in the nucleus (39). This would explain the transient nature of the interaction and subsequent separation of $RPGR^{ORF15}$ and NPM at later stages of the cell cycle.

Vertebrate photoreceptors contain an outer segment, which is a modified sensory cilium connected to the cell body by a narrow connecting cilium. Both the $RPGR^{ORF15}$ and the interacting protein RPGRIP1 have been consistently localized to ciliary axonemes in all species examined (17–18). The axoneme of connecting cilia is non-motile and projects above the basal body as a 9+0 array of microtubule doublets, corresponding to the transitional zone of motile cilia (40), to which RPGR also localizes (18). All phototransduction and structural proteins that are distributed to the outer segment are transported to the peri-ciliary ridge at the base of the connecting cilium (41), which has been proposed to correspond to the transitional fibre intra-flagellar transport docking site (42). Proteins destined for the outer segment, such as the visual pigment rhodopsin, are carried by the minus-ended microtubule-associated molecular motor cytoplasmic dynein (19), docked in the vicinity of basal bodies and further transported into the outer segments by means of plus-end directed microtubule-associated motors such as kinesin-II (20). Although centrioles are the equivalent structures to basal bodies in photoreceptors, it may be that $RPGR^{ORF15}$ plays a role in the docking of proteins at the base of the connecting cilia, as suggested by the mislocalization of opsin-containing vesicles in the *Rpgr* knockout mouse (15), and is a component of a transport complex that shuttles between the inner and outer segments along the connecting cilium. The co-localization of $RPGR^{ORF15}$ and RPGRIP1 to basal bodies in ciliated cells is consistent with this possibility.

What is the significance of the $RPGR^{ORF15}$–NPM interaction in a post-mitotic tissue such as retina? NPM was not seen in photoreceptor connecting cilia by immunohistochemistry, whereas strong labelling of nucleoli was evident. NPM was co-immunoprecipitated from extracts of total retina as well as both nuclear and ROS fractions. When whole retina and crude ROS fractions were examined for nuclear contamination with anti-RCC1 antibody, a weak band was present in ROS (Supplementary Material, Fig. S1E), suggesting that in post-mitotic retinal cells, the major RPGR–NPM interaction occurs within nuclei. There are two possible explanations. The first is that different isoforms of $RPGR^{ORF15}$ (Fig. 2E) serve different roles in nuclei and centrioles/basal bodies. NPM may be common to both by acting as a chaperone for assembling protein complexes including $RPGR^{ORF15}$. The second possibility is that both proteins are involved in the assembly of centrosomal protein complexes within nuclei, which are subsequently exported to centrosomes, as proposed for other core centrosomal proteins, because leptomycin resulted in their nuclear retention (39). Further work is required to establish the precise functions of RPGR and RPGRIP1 both in nuclei and in centrosomes but they join a growing number of centrosomal proteins implicated in human disease (43–46).

MATERIALS AND METHODS

Generation of anti-$RPGR^{ORF15}$ antibodies

Polyclonal antibodies were raised in rabbits against the bovine $ORF15^{C2}$ domain (anti-b$ORF15^{C2}$) (18) and against a synthetic peptide (^{1097}YGKHKTQKKS^{1107}) from a non-repetitive region of human $ORF15^{C2}$ (anti-h$ORF15^{1878}$) (GenBank accession nos AF286472 and AAC50481). Another peptide from the C-terminus of human ORF15 protein (1), ^{1100}HKTYQKKSVTNTQGNGKE^{1117}, was used to generate rabbit polyclonal antibody anti-$ORF15^{CP}$. The antibody was affinity-purified against the cognate peptide. Specificity of the antibodies was checked against *Escherichia coli* expressed fusion proteins and controls (Supplementary Material, Fig. S1F). The $ORF15^{CP}$ antibody identified five to six bands with apparent molecular weight range of 100–250 kDa in mammalian retinas. The bands could be abolished by pre-incubation with molar excess of the relevant peptide, but not with an unrelated peptide. In addition, the immunoreactive bands were not detected in the *Rpgr* knockout mouse retina (15) (Khanna *et al.*, unpublished data). This antibody gave the same sized bands in fractionated nuclei as anti-$ORF15^{C2}$ antibody (Fig. 2E). The anti-RPGRIP1 antibody was kindly provided by Dr Tiansen Li (26,27) and used at 1:1000 dilution.

Protein alignment

The sequences of $ORF15^{C2}$ from gorilla, rhesus monkey and marmoset, cat, rat, hamster, pig and sheep were cloned by PCR using two degenerate primers (forward: 5′-ATM CCA GAG GAR MAG GAA; reverse: 5′-CTT CAA TTC CAR RTA AWG TGG YAA. M = A|C, R = A|G, W = A|T, Y = C|T). PCR products were ligated into TOPO-TA vector (Invitrogen) and sequenced with T3 primer. The sequences of ORF15 C terminal from other species were available at NCBI (http://www.ncbi.nih.gov/). Alignment of these sequences with human $ORF15^{CT}$ was performed using CLUSTALW tool available at the European Bioinformatics Institute (http://www.ebi.ac.uk).

Constructs

GST and EGFP fusion constructs were made using the C-terminal 81 and 83 amino acids of bovine and human $RPGR^{ORF15}$ in pGEX 4T3 or pGEX 4T1 (GST tag, Amersham

Pharmacia Biotech) or EGFP-C1 (Clontech), respectively. Bacterial expression was induced with IPTG at 25°C and the supernatant purified with 50% slurry of glutathione–Sepharose 4B beads. Human NPM was expressed in pBAD-TOPO (His tag, Invitrogen) and expression induced with 0.002% arabinose at 25°C.

Yeast two-hybrid analysis

The human ORF15^{C2} construct was inserted into the pAS vector (Clontech) and transformed into the Y190 yeast strain (Yeast protocols Handbook PT3024-1). Human NPM was inserted into the pACT vector (Clontech). A colour assay for β-galactosidase activity with chlorophenol red β-D-galactopyranoside was carried out as described (Clontech Yeast Protocols Handbook PT3024-1).

Preparation of ROS extracts

Bovine retinal fractions enriched in ROS were prepared using modifications to the method of Papermaster and Dreyer (47). Briefly, one bovine retina was suspended in 1.0 ml sucrose homogenizing medium (34% sucrose, 65 mM NaCl, 2 mM $MgCl_2$, 5 mM Tris–acetate, pH 7.4) and shaken for 1 min. The resulting suspension was centrifuged at 1800*g* for 4 min and the supernatant removed into two volumes 10 mM Tris–acetate, pH 7.4. The pellet was resuspended in 1.0 ml sucrose homogenizing medium and homogenized with a loose fitting pestle, four to five passes on ice. The suspension was centrifuged at 1800*g* for 4 min, the supernatant removed into two volumes of 10 mM Tris–acetate pH 7.4 and pooled with the first supernatant. The pooled supernatants were centrifuged at 2600*g* for 4 min and the resulting pellet was designated the crude ROS extract.

Pull-down assays

The GST–ORF15^{C2} (bovine) protein was used to pull down interacting proteins from bovine retina extracts after overnight incubation at 4°C. One bovine retina (250 mg) and 250 mg bovine kidney were homogenized on ice using a Dounce homogenizer in phosphate buffered saline (PBS) containing 2% Triton X-100 and protease inhibitors and incubated by rotating at room temperature for 30 min. Tissues were further lysed by several rounds of freeze/thaw and sonication and the large debris removed by centrifugation at 10 000*g* for 20 min. The soluble supernatant was divided into two equal aliquots, one of which was incubated with bovine GST–ORF15^{C2} and the other with the GST-only vector control, each immobilized on glutathione–Sepharose 4B beads. Bound proteins were washed and removed by boiling, then separated by SDS–PAGE. Excised bands that were absent from GST-only control pull-downs were digested *in situ* with trypsin and identified by MALDI-TOF mass spectrometry or anti-NPM antibody by western blots.

In other experiments, sonicated HeLa cell extract supernatant was incubated at 4°C overnight with human and bovine EGFP–ORF15^{C2}, washed with PBS and purified on glutathione–Sepharose 4B beads prior to analysis by SDS–PAGE and western blotting with anti-NPM. Recombinant human NPM was also incubated with human GST–ORF15^{C2} and analysed as described earlier. In SDS–PAGE gels, 10 μl input extract was loaded and 200 μl used for each of the ORF15^{C2} and control pull downs.

Protein identification by mass spectrometry

Identification of NPM by peptide mass mapping utilized methods described in detail elsewhere (48,49). Briefly, gel bands were excised, destained and digested in-gel with trypsin and the resulting peptides extracted for analysis with a Voyager DE Pro MALDI-TOF mass spectrometer (PE Biosystems, Framingham, MA, USA). Measured peptide masses were used to query the Swiss-Protein, TrEMBL and NCBI sequence databases for matches using MS-Fit and Profound search programs.

Co-immunoprecipitation from cells transfected with EGFP–hORF15^{C2}

Human ORF15^{C2}, subcloned in the pEGFP vector (Clontech), and pEGFP vector control were transfected into HeLa cells using FuGENE 6 (Roche). After 3 days, the transfected HeLa cells were lysed, and anti-EGFP antibody and protein A beads were added to the lysed supernantant and incubated at 4°C overnight then washed with PBS. After boiling, the extract was subjected to SDS–PAGE followed by immunoblotting with antibody (Supplementary Material, Fig. S1G).

Co-immunoprecipitation from bovine RNE

Nuclear extracts were prepared from bovine retina and used for co-immunoprecipitation experiments as described previously (50,51). The immunoprecipitates were subjected to SDS–PAGE followed by immunoblot analysis with appropriate antibodies. The immunoblots were developed using the enhanced chemiluminescence kit (Pierce, New York, NY, USA).

Immunoblot analysis of the bovine RNE with ORF15^{CP} and ORF15^{C2} antibodies

Bovine retinal whole cell extract and nuclear extract (100–200 μg each) were subjected to SDS–PAGE followed by immunoblotting using anti-ORF15^{CP} or anti-ORF15^{C2} antibody. Equal amounts of protein were run on 7.5% (for ORF15 analysis) or 10% (all other antibodies) SDS–PAGE gels and transferred to nitrocellulose membrane. Membranes were blocked in 5% non-fat dried milk in PBS. Primary antibodies were used at 1:100 [anti-ORF15 and anti-RCC1 (BD Biosciences)] or 1:2000 for anti-NPM (a gift from Dr P.K. Chan, Chinese University of Hong Kong). Anti-rabbit (BioRad) or anti-mouse (Scottish Antibody Production Unit) HRP-conjugated secondary antibodies were used at a 1:5000 dilution. Bound antibody was visualized by ECL (Amersham Biosciences).

RT–PCR of RPGR^{ORF15}

Total RNA from cultured cells was isolated using the Micro-to-midi total RNA purification system (Invitrogen). RT–PCR was performed with the SuperScript^{TM} one-step RT–PCR kit

(Invitrogen). The following primers were used: *RPGR*^{ORF15}, 5′-GAT TCT TTT TCA ATG AGG AGA ACA -3′ and 5′-ATT TCC TTT TGA ATC CTC TGC TCC-3′; glyceraldehyde-3-phosphate dehydrogenase (*GAPD*) 5′-ATG GGG AAG GTG AAG GTC GGA-3′ and 5′-TTA CTC CTT GGA GGC CAT GTG-3′. The forward primer for *RPGR* is in exon 11, the reverse primer is near the start of exon ORF15, which results in an RT–PCR product of ∼498 bp.

Cells and transfection

COS7 cells were maintained in Dulbecco's modified Eagle medium (DMEM) supplemented with 5% fetal calf serum, penicillin (100 U/ml) and streptomycin (130 μg/ml) at 37°C in an atmosphere of 5% CO_2. Transient transfection was performed using FuGENE 6 (Roche) (6 μl) added to DNA (2.0 μg) following the manufacturer's instructions. Cells were transfected with an enhanced green fluorescent protein (EGFP) vector containing the ORF15^{C2} DNA sequence fused to the C-terminus of EGFP. After incubation for 48 h, cells were washed in PBS, fixed with ice cold methanol for 2 min at −20°C, washed in PBS, blocked with 10% normal sheep serum in PBS, then incubated with anti-NPM at 1:100 in 10% normal sheep serum for 1 h at room temperature, in a moist chamber. Cells were washed in PBS, blocked again and incubated with Texas Red-conjugated secondary antibody (Jackson Laboratories) at 1:100 in 10% normal sheep serum in PBS for 1 h at room temperature in the dark, in a moist chamber. Cells were then washed in PBS and mounted in Vectashield (Vector Laboratories Ltd) containing 4′-6-diamidino-2-phenylindole (DAPI) (1.0 μg/ml). Images were captured using an Axioplan two fluorescent microscope and analysed using IPLab software.

Mouse internal IMCD3 were purchased from American Type Culture Collection (Rockville, MD, USA) and cultured to confluence in DMEM/HAM's F12 (Gibco-BRL, Rockville, MD, USA) and supplemented with 10% fetal bovine serum (FBS) and 100 U/ml of penicillin/streptomycin in a humidified 5% CO2 incubator, maintained at 37°C.

Immunocytochemistry

COS7 cells were grown at 37°C in a 5% CO_2 atmosphere in DMEM supplemented with 10% FBS and penicillin–streptomycin (100 IU/ml and 100 μg/ml, respectively). For immunofluorescence, cells were grown on acid treated coverslips overnight before being fixed and permeabilized with −20°C methanol for 10 min. The cells were rehydrated with PBS for 10 min then blocked in PBS–1% BSA for 5 min. Cells were then incubated with the anti-ORF15^{C2} antibody (1:50, rabbit) plus anti-γ-tubulin (1:2000; Sigma, St Louis, MO, USA). The mouse primary antibodies were detected using biotin anti-mouse (Amersham) followed by incubation with Streptavidin Texas Red to detect the biotin (Amersham). The rabbit primary antibodies were detected using Alexa 488 (Molecular probes, Eugene, OR, USA) and the DNA was stained using Hoechst 33258 dye (Calbiochem, 0.2 μg/ml) for 1 min. All antibodies were diluted in PBS–3% BSA and all antibody incubations were for 45 min at room temperature. The cells were washed 3 × 5 min between each antibody incubation. Following the completion of labelling, the coverslips were mounted onto slides in 80% glycerol 3% *n*-propylgallate to prevent fading. Images were captured on a Nikon TE300 inverted microscope using an ORCA ER (Hamamatsu, Shizuoka, Japan) using Openlab 3.09 software (Improvision, Coventry, UK) and processing using Adobe Photoshop (Adobe Systems, San Jose, CA, USA).

Fluorescence staining of retinal cryosections

Immunofluorescence studies were essentially performed as previously described (52,53). Briefly, eyes from adult C57BL/6J mice were prefixed in 4% paraformaldehyde in PBS for 1 h at room temperature, washed, soaked with 30% sucrose in PBS overnight, and cryofixed in melting isopentane. Cryosections were placed on poly-L-lysine-precoated coverslips. Specimens were incubated with 50 mM NH_4Cl and 0.1% Tween-20 in PBS and blocked with blocking solution [0.5% cold-water fish gelatin (Sigma) plus 0.1% ovalbumin (Sigma) in PBS]. For double labelling, sections were incubated with a mixture of antibodies in blocking solution overnight at 4°C. In these experiments, anti-centrin antibodies were used as markers for the connecting cilium (54). The specimens were washed and subsequently incubated with secondary antibodies conjugated to Alexa® 488 or Alexa® 546 (Molecular Probes) in blocking solution for 1 h at room temperature in the dark. Washed sections were mounted in Mowiol 4.88 (Hoechst, Frankfurt, Germany) containing 2% *n*-propyl-gallate, and in the case of triple staining, 1 μg/ml 4,6-diamidino-2-phenylindole. Mounted retinal sections were examined with a Leica DMRP microscope. Images were obtained with a Hamamatsu Orca ER CCD camera (Hamamatsu city, Japan) and processed with Adobe Photoshop (Adobe Systems).

SUPPLEMENTARY MATERIAL

Supplementary Material is available at HMG Online.

ACKNOWLEDGEMENTS

We are grateful to Dr Tiansen Li (Harvard) for an RPGRIP1 antibody and for providing *Rpgr* knockout mice. We thank S. Bruce for the artwork. We acknowledge the support of the Medical Research Council (A.F.W.), Foundation Fighting Blindness (A.F.W., A.S. and J.W.C.), NIH EY006603 and EY014239 (J.W.C.), EY007961, EY007003 (A.S.), Wellcome Trust, BBSRC and AICR (A.M.F.), Research to Prevent Blindness (A.S.) and British Retinitis Pigmentosa Society (A.F.W.). A.S. is Harold F. Falls Collegiate Professor and RPB Senior Scientific Investigator and A.M.F. is a Lister Institute Research Fellow.

REFERENCES

1. Vervoort, R., Lennon, A., Bird, A.C., Tulloch, B., Axton, R., Miano, M.G., Meindl, A., Meitinger, T., Ciccodicola, A. and Wright, A.F. (2000) Mutational hot spot within a new RPGR exon in X-linked retinitis pigmentosa. *Nat. Genet.*, **25**, 462–466.
2. Vervoort, R. and Wright, A.F. (2002) Mutations of RPGR in X-linked retinitis pigmentosa (RP3). *Hum. Mutat.*, **19**, 486–500.

3. Breuer, D.K., Yashar, B.M., Filippova, E., Hiriyanna, S., Lyons, R.H., Mears, A.J., Asaye, B., Acar, C., Vervoort, R. and Wright, A.F. *et al.* (2002) A comprehensive mutation analysis of RP2 and RPGR in a North American cohort of families with X-linked retinitis pigmentosa. *Am. J. Hum. Genet.*, **70**, 1545–1554.
4. Pusch, C.M., Broghammer, M., Jurklies, B., Besch, D. and Jacobi, F.K. (2002) Ten novel ORF15 mutations confirm mutational hot spot in the *RPGR* gene in European patients with X-linked retinitis pigmentosa. *Hum. Mutat.*, **20**, 405.
5. Bader, I., Brandau, O., Achatz, H., Apfelstedt-Sylla, E., Hergersberg, M., Lorenz, B., Wissinger, B., Wittwer, B., Rudolph, G., Meindl, A. and Meitinger, T. (2003) X-linked retinitis pigmentosa: RPGR mutations in most families with definite X linkage and clustering of mutations in a short sequence stretch of exon ORF15. *Invest. Ophthalmol. Vis. Sci.*, **44**, 1458–1463.
6. Sharon, D., Sandberg, M.A., Rabe, V.W., Stillberger, M., Dryja, T.P. and Berson, E.L. (2003) RP2 and RPGR mutations and clinical correlations in patients with X-linked retinitis pigmentosa. *Am. J. Hum. Genet.*, **73**, 1131–1146.
7. Yang, Z., Peachey, N.S., Moshfeghi, D.M., Thirumalaichary, S., Chorich, L., Shugart, Y.Y., Fan, K. and Zhang, K. (2002) Mutations in the *RPGR* gene cause X-linked cone dystrophy. *Hum. Mol. Genet.*, **11**, 605–611.
8. Mears, A.J., Hiriyanna, S., Vervoort, R., Yashar, B., Gieser, L., Fahrner, S., Daiger, S.P., Heckenlively, J.R., Sieving, P.A., Wright, A.F. and Swaroop, A. (2000) Remapping of the *RP15* locus for X-linked cone-rod degeneration to Xp11.4-p21.1, and identification of a *de novo* insertion in the *RPGR* exon ORF15. *Am. J. Hum. Genet.*, **67**, 1000–1003.
9. Demirci, F.Y., Rigatti, B.W., Wen, G., Radak, A.L., Mah, T.S., Baic, C.L., Traboulsi, E.I., Alitalo, T., Ramser, J. and Gorin, M.B. (2002) X-linked cone-rod dystrophy (locus COD1): identification of mutations in RPGR exon ORF15. *Am. J. Hum. Genet.*, **70**, 1049–1053.
10. Ayyagari, R., Demirci, F.Y., Liu, J., Bingham, E.L., Stringham, H., Kakuk, L.E., Boehnke, M., Gorin, M.B., Richards, J.E. and Sieving, P.A. (2002) X-linked recessive atrophic macular degeneration from RPGR mutation. *Genomics*, **80**, 166–171.
11. Dry, K.L., Manson, F.D., Lennon, A., Bergen, A.A., van Dorp, D.B. and Wright, A.F. (1999) Identification of a 5′ splice site mutation in the *RPGR* gene in a family with X-linked retinitis pigmentosa (RP3). *Hum. Mutat.*, **13**, 141–145.
12. Iannaccone, A., Wang, X., Jablonski, M.M., Kuo, S.F., Baldi, A., Cosgrove, D., Morton, C.C. and Swaroop, A. (2004) Increasing evidence for syndromic phenotypes associated with RPGR mutations. *Am. J. Ophthalmol.*, **137**, 785–786.
13. Zhang, Q., Acland, G.M., Wu, W.X., Johnson, J.L., Pearce-Kelling, S., Tulloch, B., Vervoort, R., Wright, A.F. and Aguirre, G.D. (2002) Different RPGR exon ORF15 mutations in Canids provide insights into photoreceptor cell degeneration. *Hum. Mol. Genet.*, **11**, 993–1003.
14. Kirschner, R., Erturk, D., Zeitz, C., Sahin, S., Ramser, J., Cremers, F.P., Ropers, H.H. and Berger, W. (2001) DNA sequence comparison of human and mouse retinitis pigmentosa GTPase regulator (RPGR) identifies tissue-specific exons and putative regulatory elements. *Hum. Genet.*, **109**, 271–278.
15. Hong, D.H., Pawlyk, B.S., Shang, J., Sandberg, M.A., Berson, E.L. and Li, T. (2000) A retinitis pigmentosa GTPase regulator (RPGR)-deficient mouse model for X-linked retinitis pigmentosa (RP3). *Proc. Natl Acad. Sci. USA*, **97**, 3649–3654.
16. Hong, D.H. and Li, T. (2002) Complex expression pattern of RPGR reveals a role for purine-rich exonic splicing enhancers. *Invest. Ophthalmol. Vis. Sci.*, **43**, 3373–3382.
17. Mavlyutov, T.A., Zhao, H. and Ferreira, P.A. (2002) Species-specific subcellular localization of RPGR and RPGRIP isoforms: implications for the phenotypic variability of congenital retinopathies among species. *Hum. Mol. Genet.*, **11**, 1899–1907.
18. Hong, D.H., Pawlyk, B., Sokolov, M., Strissel, K.J., Yang, J., Tulloch, B., Wright, A.F., Arshavsky, V.Y. and Li, T. (2003) RPGR isoforms in photoreceptor connecting cilia and the transitional zone of motile cilia. *Invest. Ophthalmol. Vis. Sci.*, **44**, 2413–2421.
19. Tai, A.W., Chuang, J-Z., Bode, C., Wolfrum, U. and Sung, C-H. (1999) Rhodopsin's carboxy-terminal cytoplasmic tail act as a membrane receptor for cytoplasmic dynein by binding the dynein light chain Tctex-1. *Cell*, **97**, 877–887.
20. Marszalek, J.R., Liu, X., Roberts, E.A., Chiu, D., Marth, J.D., Williams, D.S. and Goldstein, L.S.B. (2000) Genetic evidence for selective transport of opsin and arrestin by kinesin-II in mammalian photoreceptors. *Cell*, **102**, 172–187.
21. Meindl, A., Dry, K., Herrmann, K., Manson, F., Ciccodicola, A., Edgar, A., Carvalho, M.R., Achatz, H., Hellebrand, H., Lennon, A. *et al.* (1996) A gene (*RPGR*) with homology to the *RCC1* guanine nucleotide exchange factor is mutated in X-linked retinitis pigmentosa (RP3). *Nat. Genet.*, **13**, 35–42.
22. Roepman, R., van Duijnhoven, G., Rosenberg, T., Pinckers, A.J., Bleeker-Wagemakers, L.M., Bergen, A.A., Post, J., Beck, A., Reinhardt, R., Ropers, H.H. *et al.* (1996). Positional cloning of the gene for X-linked retinitis pigmentosa 3: homology with the guanine-nucleotide-exchange factor RCC1. *Hum. Mol. Genet.*, **5**, 1035–1041.
23. Renault, L., Nassar, N., Vetter, I., Becker, J., Klebe, C., Roth, M. and Wittinghofer, A. (1998) The 1.7 A crystal structure of the regulator of chromosome condensation (RCC1) reveals a seven-bladed propeller. *Nature*, **392**, 97–101.
24. Boylan, J.P. and Wright, A.F. (2000) Identification of a novel protein interacting with RPGR. *Hum. Mol. Genet.*, **9**, 2085–2093.
25. Roepman, R., Bernoud-Hubac, N., Schick, D.E., Maugeri, A., Berger, W., Ropers, H.H., Cremers, F.P. and Ferreira, P.A. (2000) The retinitis pigmentosa GTPase regulator (RPGR) interacts with novel transport-like proteins in the outer segments of rod photoreceptors. *Hum. Mol. Genet.*, **9**, 2095–2105.
26. Hong, D.H., Yue, G., Adamian, M. and Li, T. (2001) Retinitis pigmentosa GTPase regulator (RPGR)-interacting protein is stably associated with the photoreceptor ciliary axoneme and anchors RPGR to the connecting cilium. *J. Biol. Chem.*, **276**, 12091–12099.
27. Zhao, Y., Hong, D.-H., Pawlyk, B., Yue, G., Adamian, M., Grynberg, M., Godzik, A. and Li, T. (2003) The retinitis pigmentosa GTPase regulator (RPGR)-interacting protein: subserving RPGR function and participating in disk morphogenesis. *Proc. Natl Acad. Sci. USA*, **100**, 3965–3970.
28. Dryja, T.P., Adams, S.M., Grimsby, J.L., McGee, T.L., Hong, D.H., Li, T., Andreasson, S. and Berson, E.L. (2001) Null RPGRIP1 alleles in patients with Leber congenital amaurosis. *Am. J. Hum. Genet.*, **68**, 1295–1298.
29. Gerber, S., Perrault, I., Hanein, S., Barbet, F., Ducroq, D., Ghazi, I., Martin-Coignard, D., Leowski, C., Homfray, T., Dufier, J.L. *et al.* (2001) Complete exon-intron structure of the RPGR-interacting protein (*RPGRIP1*) gene allows the identification of mutations underlying Leber's congenital amaurosis. *Eur. J. Hum. Genet.*, **9**, 561–571.
30. Hameed, A., Abid, A., Aziz, A., Ismail, M., Mehdi, S.Q. and Khaliq, S. (2003) Evidence of *RPGRIP1* gene mutations associated with recessive cone-rod dystrophy. *J. Med. Genet.*, **40**, 616–619.
31. Schmidt-Zachmann, M.S. and Franke, W.W. (1988) DNA cloning and amino acid sequence determination of a major constituent protein of mammalian nucleoli. Correspondence of the nucleoplasmin-related protein NO38 to mammalian protein B23. *Chromosoma*, **96**, 417–426.
32. Okuda, M., Horn, H.F., Tarapore, P., Tokuyama, Y., Smulian, A.G., Chan, P.K., Knudsen, E.S., Hofmann, I.A., Snyder, J.D., Bove, K.E. *et al.* (2000) Nucleophosmin/B23 is a target of CDK2/cyclin E in centrosome duplication. *Cell*, **103**, 127–140.
33. Dammermann, A. and Merdes, A. (2002) Assembly of centrosomal proteins and microtubule organization depends on PCM-1. *J. Cell Biol.*, **159**, 255–266.
34. Wolfrum, U., Giessl, A. and Pulvermuller, A. (2002) Centrins, a novel group of Ca^{2+}-binding proteins in vertebrate photoreceptor cells. *Adv. Exp. Med. Biol.*, **514**, 155–178.
35. Doxsey, S. (2001) Re-evaluating centrosome function. *Nat. Rev. Mol. Cell Biol.*, **2**, 688–698.
36. Okuda, M. (2002) The role of nucleophosmin in centrosome duplication. *Oncogene*, **21**, 6170–6174.
37. Hingorani, K., Szebeni, A. and Olson, M.O. (2000) Mapping the functional domains of nucleolar protein B23. *J. Biol. Chem.*, **275**, 24451–24457.
38. Zatsepina, O.V., Rousselet, A., Chan, P.K., Olson, M.O., Jordan, E.G. and Bornens, M. (1999) The nucleolar phosphoprotein B23 redistributes in part to the spindle poles during mitosis. *J. Cell Sci.*, **112**, 455–466.
39. Cha, H., Hancock, C., Dangi, S., Maiguel, D., Carrier, F. and Shapiro, P. (2004) Phosphorylation regulates nucleophosmin targeting to the centrosome during mitosis as detected by cross-reactive phosphorylation-specific MKK1/MKK2 antibodies. *Biochem. J.*, **378**, 857–865.
40. Rohlich, P. (1975) The sensory cilium of retinal rods is analogous to the transitional zone of motile cilia. *Cell Tissue Res.*, **161**, 421–430.

41. Deretic, D. and Papermaster, D.S. (1991) Polarized sorting of rhodopsin on post-Golgi membranes in frog retinal photoreceptor cells. *J. Cell Biol.*, **113**, 1281–1293.
42. Deane, J.A., Cole, D.G., Seeley, E.S., Diener, D.R. and Rosenbaum, J.L. (2001) Localization of intraflagellar transport protein IFT52 identifies basal body transitional fibers as the docking site for IFT particles. *Curr. Biol.*, **11**, 1586–1590.
43. Nurnberger, J., Kribben, A., Saez, A.O., Heusch, G., Philipp, T. and Phillips. C.L. (2004) The *Invs* gene encodes a microtubule-associated protein. *J. Am. Soc. Nephrol.*, **15**, 1700–1710.
44. Swaminathan, S. (2004) Human disease: the centrosome connection. *Nat. Cell Biol.*, **6**, 383.
45. Ansley, S.J., Badano, J.L., Blacque, O.E., Hill, J., Hoskins, B.E., Leitch, C.C., Kim, J.C., Ross, A.J., Eichers, E.R., Teslovich, T.M. *et al.* (2003) Basal body dysfunction is a likely cause of pleiotropic Bardet-Biedl syndrome. *Nature*, **425**, 628–633.
46. Romio, L., Fry, A.M., Winyard, P.J.D., Malcolm, S., Woolf, A.S. and Feather, S.A. (2004) OFD1 is a centrosomal/basal body protein expressed during mesenchymal-epithelial transition in human nephrogenesis. *J. Am. Soc. Nephrol.*, **15**, 2556–2568.
47. Papermaster, D.S. and Dreyer, W.J. (1974) Rhodopsin content in the outer segment membranes of bovine and frog retinal rods. *Biochemistry*, **13**, 2438–2444.
48. Miyagi, M., Sakaguchi, H., Darrow, R.M., Yan, L., West, K.A., Aulak, K.S., Stuehr, D.J., Hollyfield, J.G., Organisciak, D.T. and Crabb, J.W. (2002) Evidence that light modulates protein nitration in rat retina. *Mol. Cell. Proteomics*, **1**, 293–303.
49. West, K.A., Yan, L., Shadrach, K., Sun, J., Hasan, A., Miyagi, M., Crabb, J.S., Hollyfield, J.G., Marmorstein, A.D. and Crabb, J.W. (2003) Protein database, human retinal pigment epithelium. *Mol. Cell. Proteomics*, **2**, 37–49.
50. Mitton, K.P., Swain, P.K., Khanna, H., Dowd, M., Apel, I.J. and Swaroop, A. (2003) Interaction of retinal bZIP transcription factor NRL with Flt3-interacting zinc-finger protein Fiz1: possible role of Fiz1 as a transcriptional repressor. *Hum. Mol. Genet.*, **12**, 365–373.
51. Cheng, H., Khanna, H., Oh, E.C., Hicks, D., Mitton, K.P. and Swaroop, A. (2004) Photoreceptor-specific nuclear receptor NR2E3 functions as a transcriptional activator in rod photoreceptors. *Hum. Mol. Genet.*, **13**, 1563–1575.
52. Wolfrum, U. and Schmitt, A. (2000) Rhodopsin transport in the membrane of the connecting cilium of mammalian photoreceptor cells. *Cell Motil. Cytoskeleton*, **46**, 95–107.
53. Pulvermüller, A., Gießl, A., Heck, M., Wottrich, R., Schmitt, A., Ernst, O.P., Choe, H-W., Hofmann, K.P. and Wolfrum, U. (2002) Calcium dependent assembly of centrin/G-protein complex in photoreceptor cells. *Mol. Cell. Biol.*, **22**, 2194–2203.
54. Wolfrum, U., Gießl, A. and Pulvermüller, A. (2002) Centrins in vertebrate photoreceptor cells. *Adv. Exp. Med. Biol.*, **514**, 179–203.